Self-assembling Multidomain Peptides: Design and Characterization of Neutral Peptide-based Materials with pH and Ionic Strength Independent Self-Assembly

Tania L. Lopez-Silva, [†] *David G. Leach,* [†] *I-Che Li,* [†] *Xinran Wang,* [†] *Jeffrey D. Hartgerink**[†‡]

[†]Department of Chemistry and [‡]Department of Bioengineering, Rice University, Houston, Texas 77005, United States

Supporting Information

Table of Contents

Table S1: $O_n(SL)_6O_n$ peptide series and control peptides S3

Figure S1: MALDI TOF MS of $O_n(SL)_6O_n$ series S4

Table S2: Estimation of the secondary structure of O series peptides S5

Figure S2: Basis spectra for CD spectroscopy data fitting S5

Table S3: Regression estimator coefficients of the least square linear method S6

Figure S3: Experimental and fit CD spectra S6

Figure S4: Effect of TFE in the secondary structure of $K_2(SL)_6K_2$ 1 wt. % solutions S7

Figure S5: Effect of TFE in the secondary structure of $O_5(SL)_6O_5$ 1 wt. % solutions S7

Figure S6: Negative-stained TEM images of $O_n(SL)_6O_n$ dissolved initially TFE S8

Figure S7: Viscoelastic properties of $O_5(SL)_6O_5$ peptide hydrogel at 1 wt.% in PBS S9

Figure S8: Inverted-vial test of $K_2(SL)_6K_2$, $O_5(SL)_6O_5$ and $E_2(SL)_6E_2$ gels S9

Figure S9: Frequency sweep of $O_5(SL)_6O_5$ peptide hydrogel S10

Figure S10: NIH-3T3 fibroblasts cultured in 1 wt.% O_5 recover from encapsulation S10

Figure S11: H&E staining of $O_5(SL)_6O_5$ implants S11

Figure S12: Masson's Trichome of $O_5(SL)_6O_5$ implants S12

References S12

Table S1. $O_n(SL)_6O_n$ series and control peptides

Peptide				
Name	**Sequence**	**Monoisotopic mass (Da)**	**Molecular weight (Da)**	**Molar concentration of 1wt.% solutions**
O_1	Ac-OSLSLSLSLSLSLO-$CONH_2$	1485.83	1486.71	6.7 mM
O_2	Ac-OOSLSLSLSLSLSLOO-$CONH_2$	1711.93	1712.94	5.8 mM
O_3	Ac-OOOSLSLSLSLSLSLOOO-$CONH_2$	1938.04	1939.17	5.1 mM
O_4	Ac-OOOOSLSLSLSLSLSLOOOO-$CONH_2$	2164.15	2165.41	4.6 mM
O_5	Ac-OOOOOSLSLSLSLSLSLOOOOO-$CONH_2$	2390.25	2391.64	4.2 mM
O_6	Ac-OOOOOOSLSLSLSLSLSLOOOOOO-$CONH_2$	2616.35	2617.87	3.8 mM
K_2	Ac-KKSLSLSLSLSLSLKK-$CONH_2$	1772.10	1773.17	5.6 mM
E_2	Ac-EESLSLSLSLSLSLEE-$CONH_2$	1775.89	1776.94	5.6 mM
$(Hyp)_6$	Ac-OOOOOO-$CONH_2$	737.34	737.75	1.4 mM

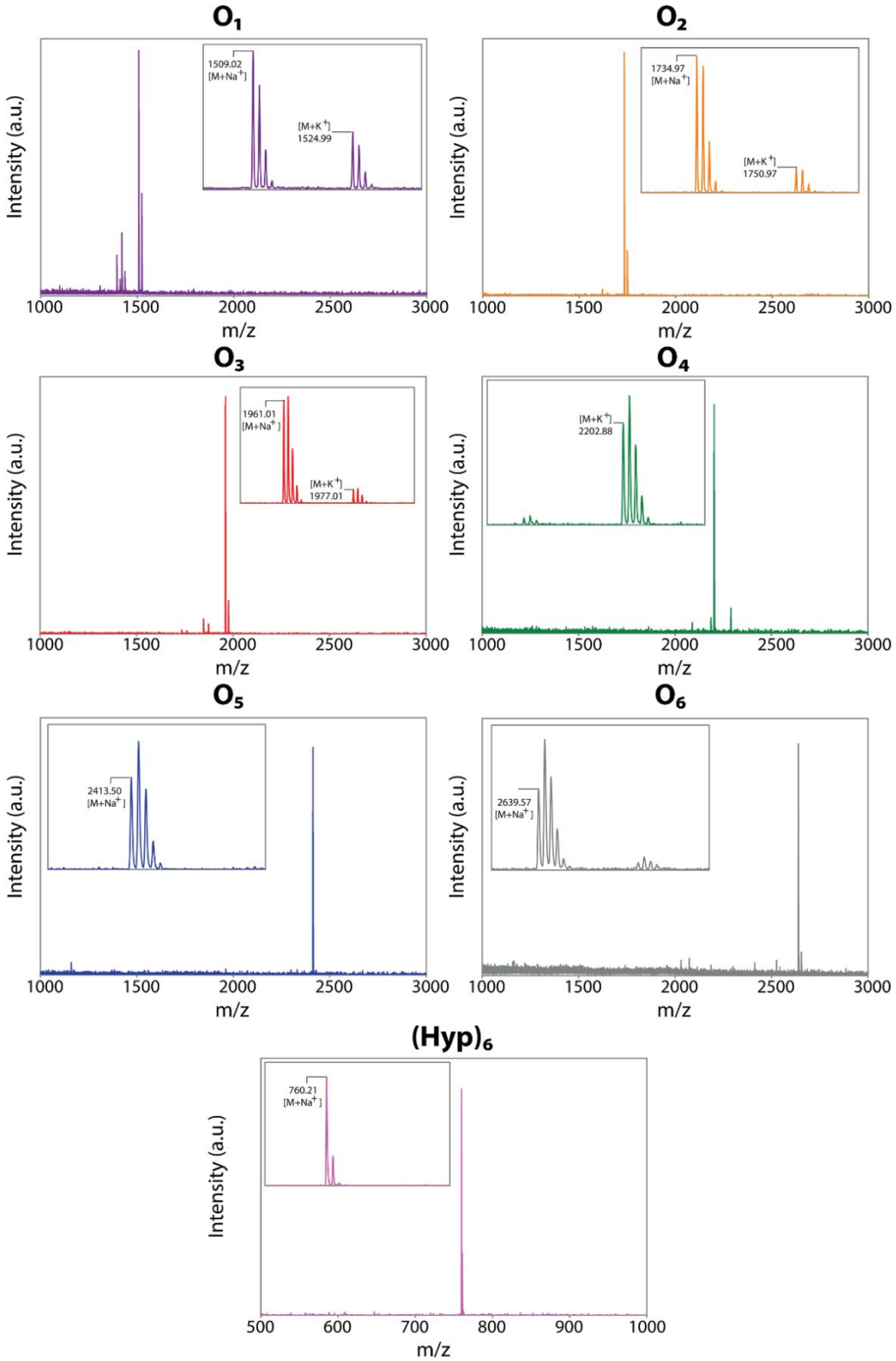

Figure S1: MALDI TOF MS of $O_n(SL)_6O_n$ series.

Table S2. Estimation of the secondary structure of O series peptides in TFE at 25°C from circular dichroism data using the least square linear method.

	TFE				
Peptide	**% ppII[a]**	**% β-sheet[a]**	**% α-helix[a]**	**nmrsd[b]**	**Predominant structure**
O_1	0	100	0	2.7×10^{-15}	β-sheet
O_2	29.3	28.8	41.9	1.53	α-helix
O_3	38.4	25.2	36.4	0.39	PPII/ α-helix
O_4	41.8	17	41.2	0.25	PPII/ α-helix
O_5	50	9.5	40.5	0.08	PPII
O_6	48.5	11.4	40.2	0.05	PPII

[a] Percentage of each structure was calculated from the regression estimator coefficients (SI Table S3, Figure S3). Basis spectra for the determination of peptide secondary structure were: O_1 for β-sheet, $(Hyp)_6$ for polyproline type II and K_2 for α-helix (SI Figure S2).
[b] nmrsd is normalized root square deviation.

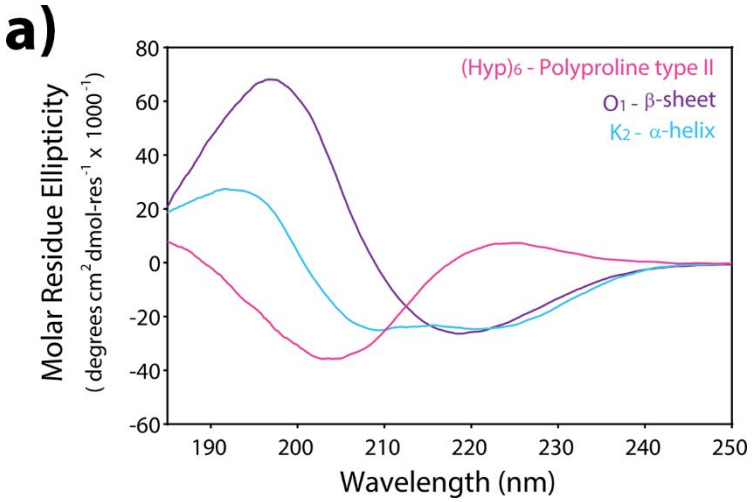

Figure S2: Basis spectra for CD spectroscopy data fitting in a) 2,2,2-trifluoroethanol (TFE) 1 wt. % solutions. TFE is well-known to promote α-helical structure in peptide and proteins. [1–3]

Table S3: Regression estimator coefficients of the analysis of peptide solutions in TFE by the least square linear method (β-sheet, PPII, α-helix).

Peptide	β-sheet	PPII	α-helix	rms[a]	nmrsd[b]
O1	1	0	0	0	0
O2	0.59	0.60	0.86	36.31	1.53
O3	0.36	0.55	0.52	19.24	0.39
O4	0.26	0.64	0.63	23.12	0.25
O5	0.12	0.63	0.51	9.58	0.08
O6	0.15	0.64	0.53	5.78	0.05

[a] rms: root mean square
[b] nmrsd: normalized root square deviation

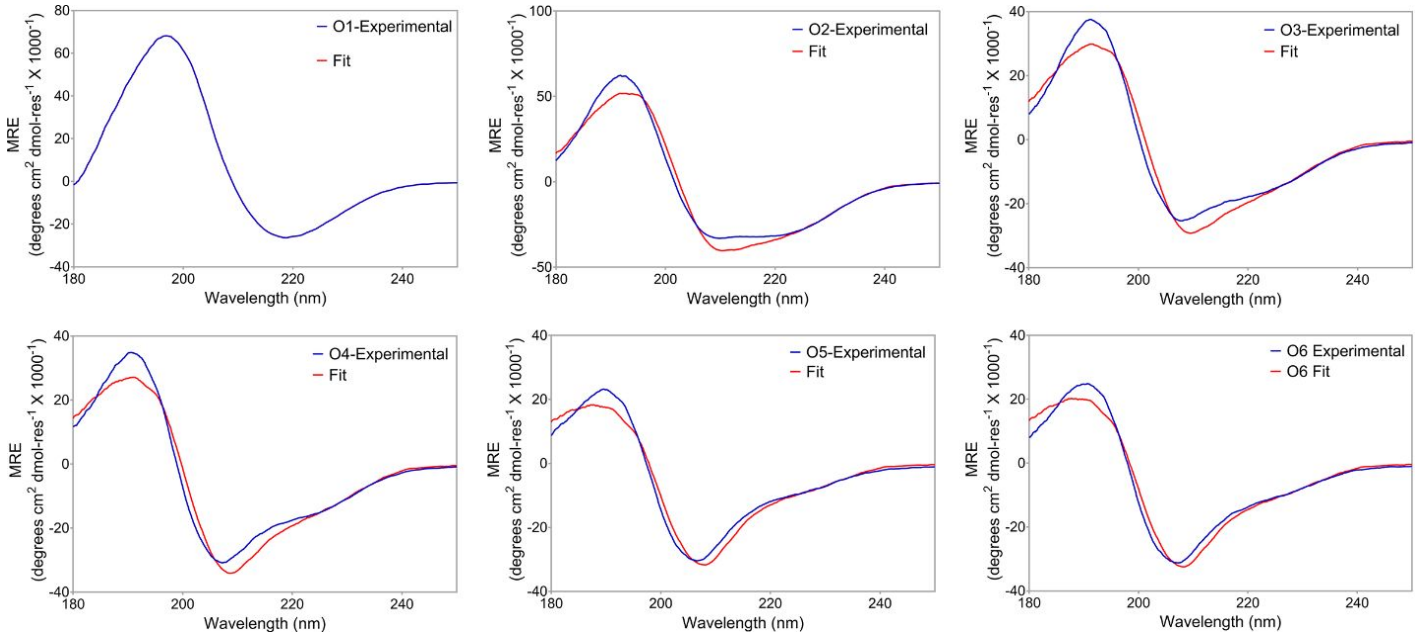

Figure S3: CD spectroscopy of 1 wt % solutions dissolved in 2,2,2-trifluoroethanol and their fits.

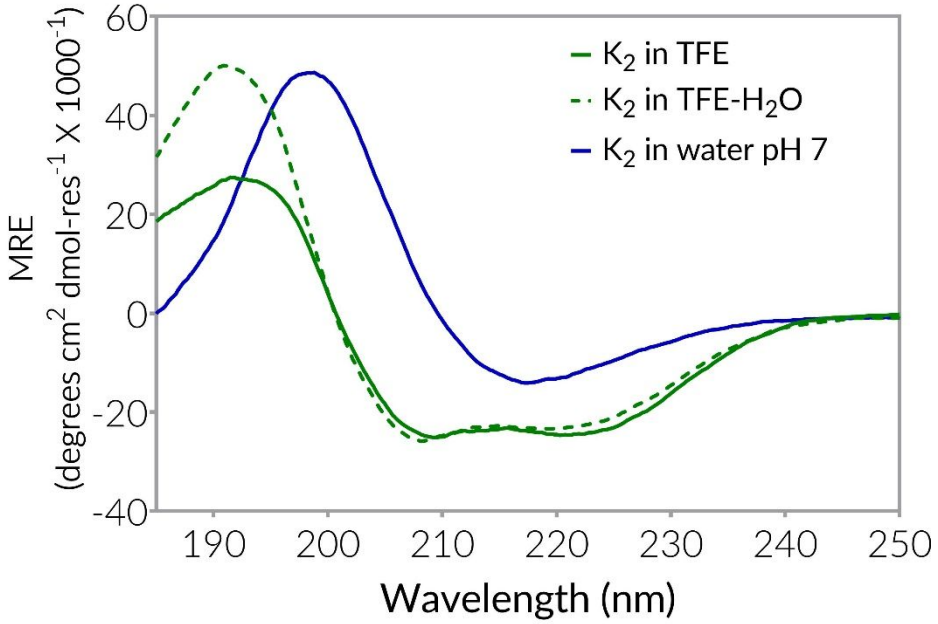

Figure S*4*: Circular Dichroism spectra of $K_2(SL)_6K_2$ at 1 wt. % in different solvents. The peptide has a canonical β-sheet structure in water at pH 7 but changes to a canonical α-helix in the presence of TFE.

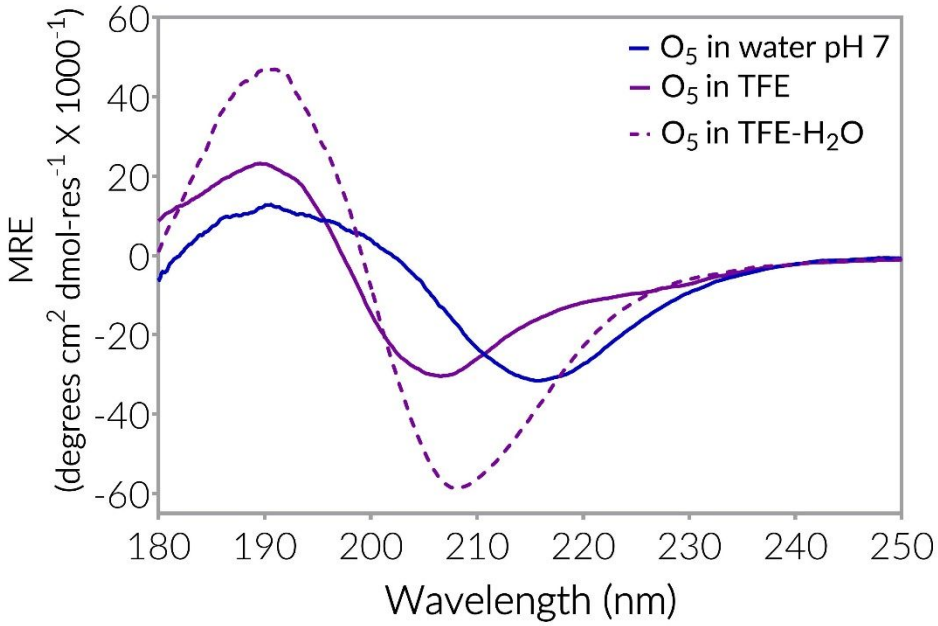

Figure S5: Circular Dichroism spectra of $O_5(SL)_6O_5$ at 1 wt. % in different solvents.

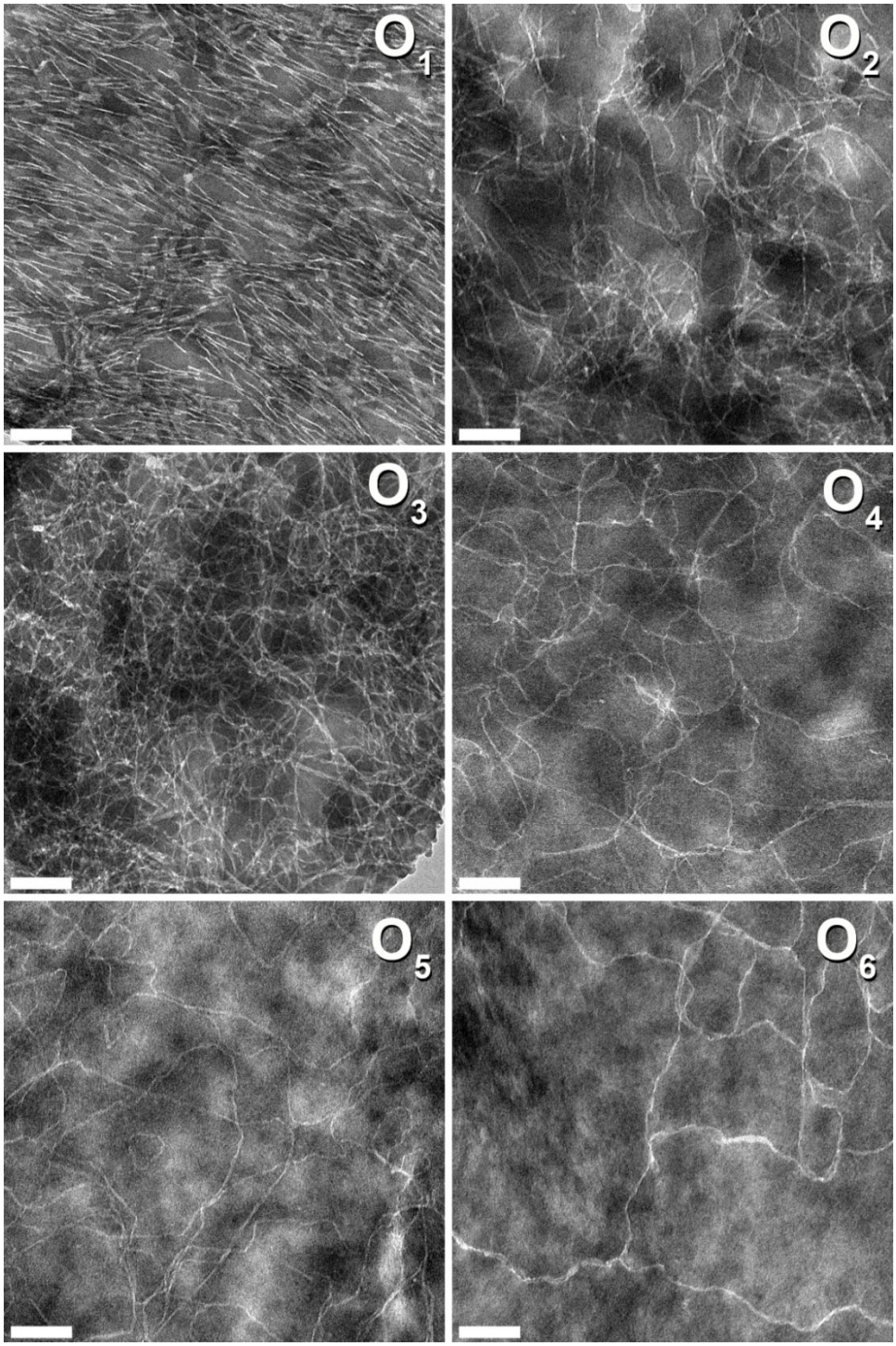

Figure *S6.* Negative-stained TEM images of $O_n(SL)_6O_n$ dissolved initially in 2,2,2-trifluoroethanol (TFE) at 1wt.% and diluted with water to final concentration. O_1 at 0.001 wt.%, O_2, O_3, O_4, O_5 and O_6 at 0.01 wt.%. Scale bar =100 nm.

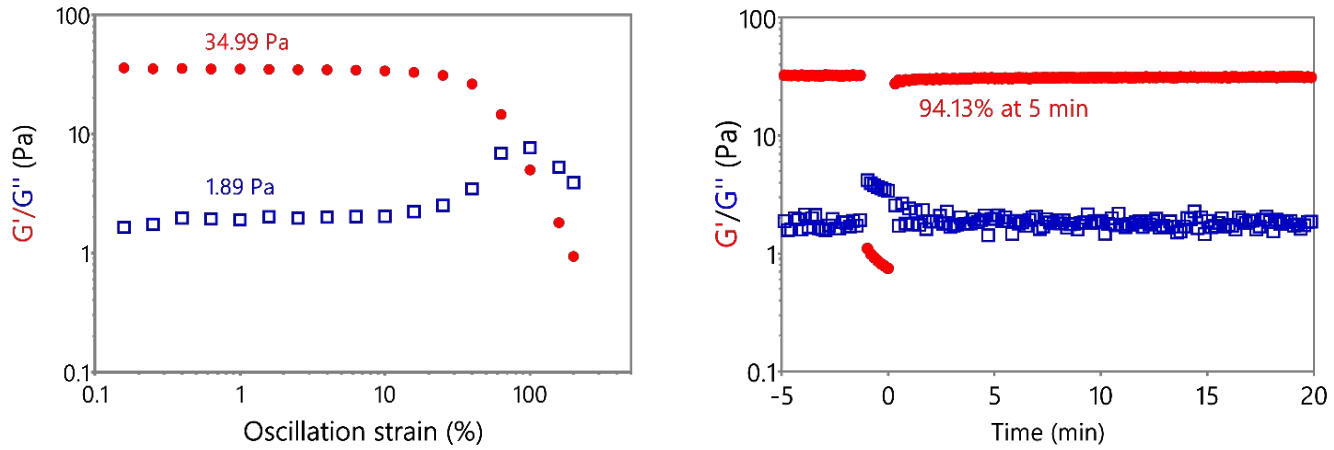

Figure S7: Viscoelastic properties of $O_5(SL)_6O_5$ peptide hydrogel at 1 wt.% in PBS (5 mM phosphate and 150 mM NaCl).

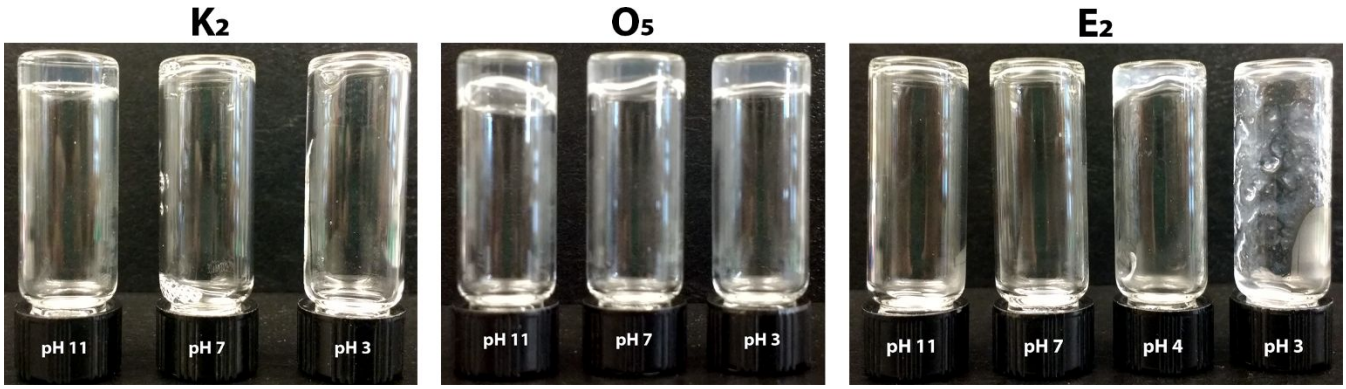

Figure S8: Inverted-vial test of $K_2(SL)_6K_2$, $O_5(SL)_6O_5$ and $E_2(SL)_6E_2$ peptide solutions/hydrogel at acidic, neutral and basic pH. Positively charged MPD (K_2) forms a gel at pH 11, negatively charged MDP (E_2) forms a gel at acidic pH and undergoes phase separation. Neutral MDP (O_5) remains a hydrogel at all pH and without the presence of multivalent ions.

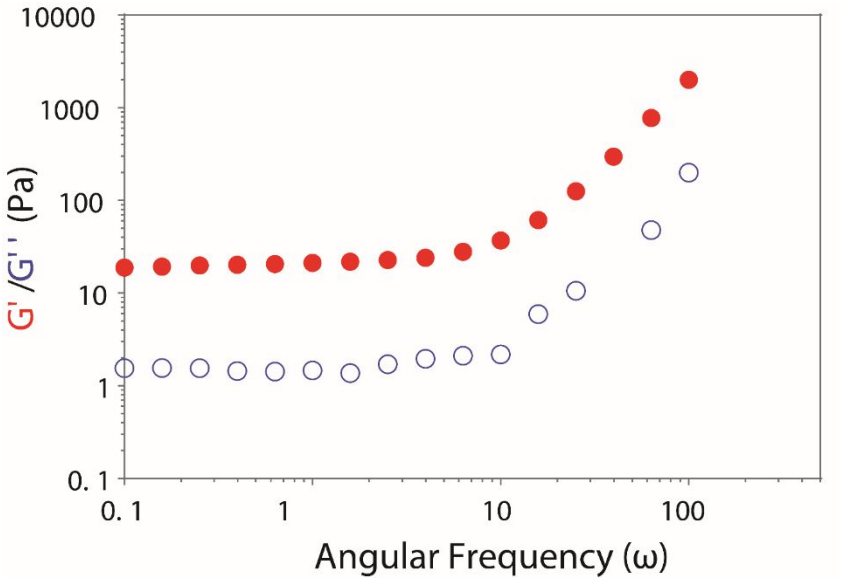

Figure S9: Frequency sweep of $O_5(SL)_6O_5$ peptide hydrogel at 1 wt. % in 149 mM sucrose and 0.5X HBSS.

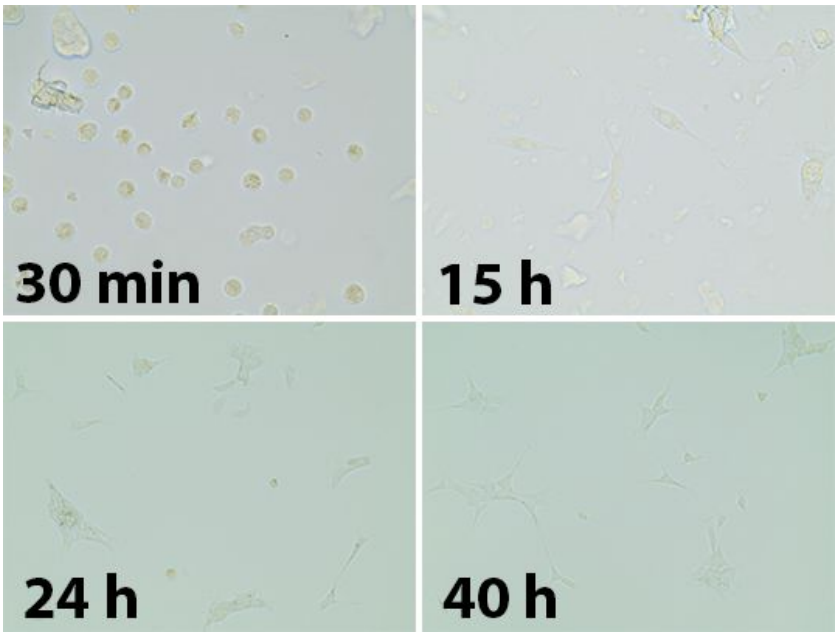

Figure S10. NIH-3T3 fibroblasts cultured in 1 wt.% O_5 for 5 days grow and proliferate again after harvesting from the peptide scaffold. 30 min after harvesting, the cells are still in the balled-up morphology, but they start adhering to the tissue plastic and recover.

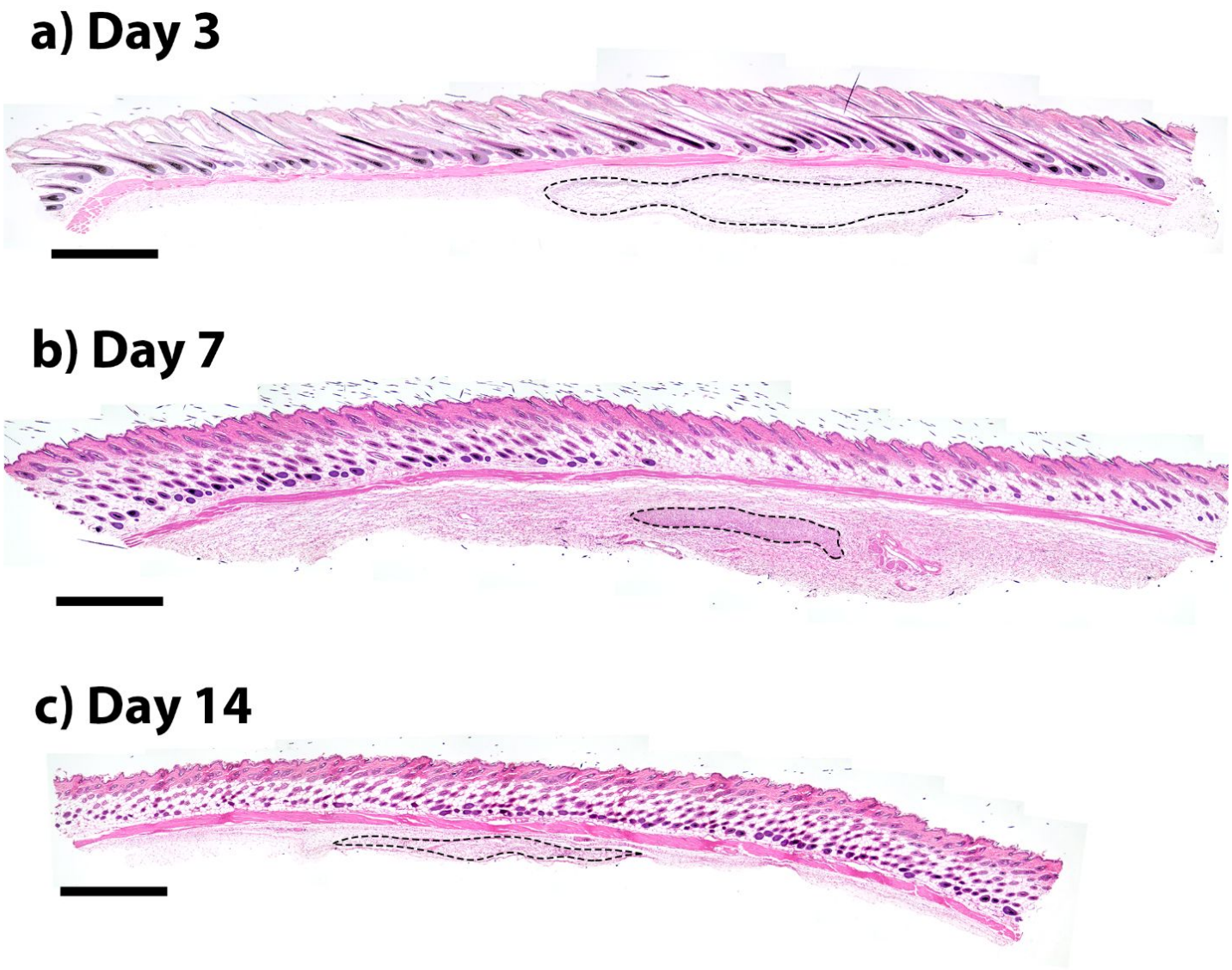

Figure S11: H&E staining of $O_5(SL)_6O_5$ implants at day a) 3, b) 7 and c)14 after injection in a subcutaneous mouse model. Implant is degraded over time and size decreases. Scale bar: 1 mm.

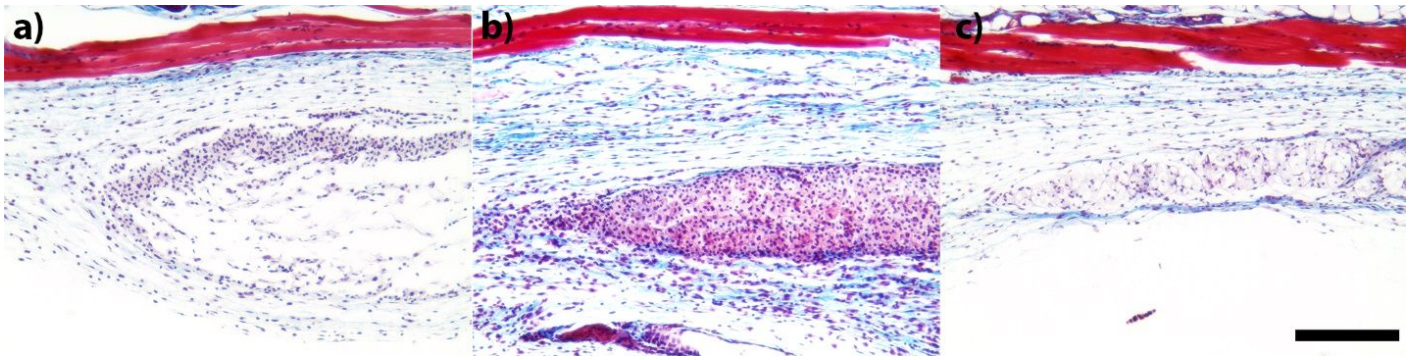

Figure S*12*: Masson's Trichome of $O_5(SL)_6O_5$ implants at day a) 3, b) 7 and c)14 after injection in a subcutaneous mouse model. The material is degraded and replaced by collagen similar to native tissue. Scale bar: 100 µm.

References:

(1) Roccatano, D.; Colombo, G.; Fioroni, M.; Mark, A. E. Mechanism by Which 2,2,2-Trifluoroethanol/Water Mixtures Stabilize Secondary-Structure Formation in Peptides: A Molecular Dynamics Study. *Proc. Natl. Acad. Sci.* **2002**, *99* (19), 12179–12184. DOI: 10.1073/pnas.182199699

(2) Myers, J. K.; Pace, C. N.; Scholtz, J. M. Trifluoroethanol Effects on Helix Propensity and Electrostatic Interactions in the Helical Peptide from Ribonuclease T1. *Protein Sci.* **1998**, *7* (2), 383–388. DOI: 10.1002/pro.5560070219

(3) SÖnnichsen, F. D.; Van Eyk, J. E.; Hodges, R. S.; Sykes, B. D. Effect of Trifluoroethanol on Protein Secondary Structure: An NMR and CD Study Using a Synthetic Actin Peptide. *Biochemistry* **1992**, *31* (37), 8790–8798. DOI: 10.1021/bi00152a015